

# Influence of Backbone Solvation on Small Angle Neutron Scattering from Polyelectrolyte Solutions

Brett D. Ermi

Department of Chemistry, University of Southern California,  
Los Angeles, California 90089-0482

Eric J. Amis\*

Polymers Division, National Institute of Standards and Technology,  
Gaithersburg, Maryland 20899

Received April 9, 1997; Revised Manuscript Received July 23, 1997\*

**ABSTRACT:** Recent theoretical and experimental studies of polyelectrolyte solutions have suggested that hydrophobic interactions between the chain backbone and the solvent lead to some of the essential observations of polyelectrolyte solution scattering. In the current paper we present small angle neutron scattering data on a polyelectrolyte, poly(*N*-methyl-2-vinylpyridinium chloride) dissolved in ethylene glycol where the hydrophobic effect is not present. This system shows the same general pattern, a peak at finite wavevector and steep upturn at low wavevector, as for those having hydrophobic interactions so that the influences of poor backbone solvation appear to be unessential for explaining the characteristics of polyelectrolyte scattering data. We demonstrate that in the scattering from polyelectrolytes after the addition of salt, the unusual peak and steep upturn are suppressed and the scattering parallels scattering from the neutral chains.

## Introduction

Polyelectrolytes and ion-containing polymers are an intriguing class of polymers with broad scientific and technological appeal.<sup>1</sup> They are crucial to biological function, essential in many modern materials and processes, and scientifically fascinating due to their variability of properties. As a result, polyelectrolytes have been the focus of decades of theoretical and experimental investigation with progress made in many areas. Despite this progress, we still lack clear molecular interpretations for most of their properties.<sup>2</sup>

Over the past 20 years there has been continuing interest in scattering experiments on low ionic strength polyelectrolyte solutions.<sup>3–19</sup> In particular, small angle neutron scattering (SANS) and small angle X-ray scattering (SAXS) studies on polyelectrolyte solutions have resulted in many unexpected results.<sup>4–6,9,12,13,15–19</sup> SANS studies from neutral polymer solutions reveal intensity profiles which are monotonically decreasing functions of scattering angle.<sup>20</sup> However, SANS studies from polyelectrolyte solutions show a peak in the angular dependence of the scattered intensity along with a steep upturn at very low angles.<sup>4–6,13,16–18</sup> The maximum has received much attention, being interpreted with several models, yet none has been completely accepted by the scientific community. Moreover, the excess scattering at low  $q$  has received little attention in the literature.

A further complication for aqueous solutions concerns backbone solvation. Generally, polyelectrolyte systems considered previously have consisted of polymers with hydrophobic backbones, such as styrene or other vinyl-based polymers, modified with pendant ionic groups to impart solubility in water. For weakly charged systems, it is expected that as the solvent quality for the chain backbone decreases, macroscopic phase separation will occur. However, it was recently shown theoretically that the presence of a small amount of charged groups inhibits large scale demixing and favors microscopic

phase separation into oppositely charged polymer-rich and polymer-poor domains.<sup>21,22</sup> This has its origin in the large entropic contributions from counterions and overall electroneutrality requirements. In these studies, hydrophobic forces favor macroscopic demixing, but because electroneutrality must be preserved, counterions would be forced out of solution into the polymer phase at a large entropic cost. The prediction is that a stable mesophase will develop as a result of these competing forces. Thus, a maximum in the solution structure factor centered at a finite  $q$  value is expected, reflecting the characteristic length scale of the microphase separation.

Borue and Erukhimovich (BE) calculated a structure factor based on this model,<sup>21</sup> and it has been used in the analysis of recent SANS experiments.<sup>15,18</sup> Moussaid et al.<sup>15</sup> studied the structure factor of aqueous solutions of a weakly charged polyelectrolyte, poly(acrylic acid), and observed a maximum in the scattering function for solutions at room temperature. Shibayama and Tanaka<sup>18</sup> also reported SANS from weakly charged polyelectrolyte solutions. Their studies on aqueous solutions of poly(*N*-isopropylacrylamide-*co*-acrylic acid) show a maximum in the scattering function above a temperature approximately equal to the lower critical solution temperature. Both groups have analyzed their data under the framework of the BE model. The calculated scattering function fits the data of Moussaid et al. quite well, while Shibayama and Tanaka observe a steep upturn at low  $q$ , which is attributed to incipient macroscopic phase separation. If this contribution was arbitrarily subtracted from the scattering function, the BE model fits the data adequately.

For chains with higher charge densities, it is unclear how the hydrophobic nature of the backbone continues to contribute to the overall physics of the system. Recently, it was shown<sup>19</sup> that for aqueous solutions of a hydrophilic backbone polyelectrolyte, the position of the broad peak in the structure factor is virtually independent of charge density from 30% to 100%, where a 100% charge density indicates that every monomer

\* Abstract published in *Advance ACS Abstracts*, October 1, 1997.

possesses an ionizable group. However, for aqueous solutions of a hydrophobic backbone polyelectrolyte, the peak position is a continuous function of charge density from 30% to 100%. The authors proposed that hydrophobic interactions must be considered, even for highly charged polyelectrolytes.

For the present work, a polyelectrolyte and solvent have been chosen, poly(*N*-methyl-2-vinylpyridinium chloride) (PMVP) and ethylene glycol (EG), which are free of backbone-solvent hydrophobic interactions.<sup>23</sup> Previous dynamic light scattering measurements on this system<sup>24</sup> showed two dynamic modes with strong dependence on added salt, which is typical for aqueous polyelectrolyte solutions. Ethylene glycol has  $pK_a$  and hydrogen bonding interactions that mimic water. Its dielectric constant of 37.7 is approximately half that of water (78.5) but still higher than most organic solvents. For this work, PMVP is studied by SANS in deuterated EG to determine the extent to which the polyelectrolyte effects observed in low ionic strength solutions are influenced by backbone solvation. For comparison, the SANS investigations were extended to the neutral chain poly(2-vinylpyridine) in the same solvent and a more traditional system where hydrophobic interactions are possible, PMVP in  $D_2O$ .

## Experimental Section

The details of the polymer preparation were described previously.<sup>24</sup> Briefly, anionically polymerized poly(2-vinylpyridine) (PVP) ( $M_w = 281\,000$  g/mol;  $M_w/M_n = 1.03$ ) obtained from Pressure Chemical<sup>25</sup> was partially quaternized with dimethyl sulfate in dimethylformamide at room temperature.<sup>34</sup> The degree of quaternization for the polymers used in this study is 45% as measured by standard titration of the chloride counterion. Ethylene glycol- $d_6$  (Cambridge Isotopes, 99% D) and deuterated water ( $D_2O$ , Cambridge Isotopes, 99.9% D, low paramagnetic) were used as received.

Small angle neutron scattering measurements were performed on the 8 m SANS facility of the Cold Neutron Research Facility at the National Institute of Standards and Technology. The neutron beam was monochromated to 9 Å with a velocity selector having a wavelength spread of 0.25 ( $\Delta\lambda/\lambda = 0.25$ ). The scattered neutrons were detected by a 64 cm × 64 cm two-dimensional detector with a sample to detector distance of 3.6 m. This configuration allows for  $q$  values in the range  $0.008 < q (\text{\AA}^{-1}) < 0.089$ , where  $q$  is the scattering vector defined as  $q = (4\pi/\lambda_0) \sin(\theta/2)$ , with  $\lambda_0$  the neutron wavelength and  $\theta$  the scattering angle. The resulting data were corrected for background electronic noise, detector inhomogeneity, empty cell scattering, and solvent scattering. The intensities were scaled to absolute intensities using an external silica standard following correction for sample transmission. The uncertainties of the individual data points for the  $I(q)$  versus  $q$  plots are calculated statistically from the number of averaged detector counts. For the plots displayed in this publication, the standard uncertainties are less than the size of the data points and are not shown. The position of the maximum,  $q_{\text{max}}$ , was determined with a standard uncertainty of  $\pm 1 \times 10^{-4} \text{\AA}^{-1}$  using a Lorentzian function fit to the data. (All uncertainty values reported in this publication are for one standard deviation.)

## Results and Discussion

Figure 1 shows the SANS intensity profiles of PVP in EG- $d_6$  for three different concentrations of polymer from 1.2 to 10 g/L. Each are monotonically decreasing functions of  $q$ , as is expected for these neutral polymer

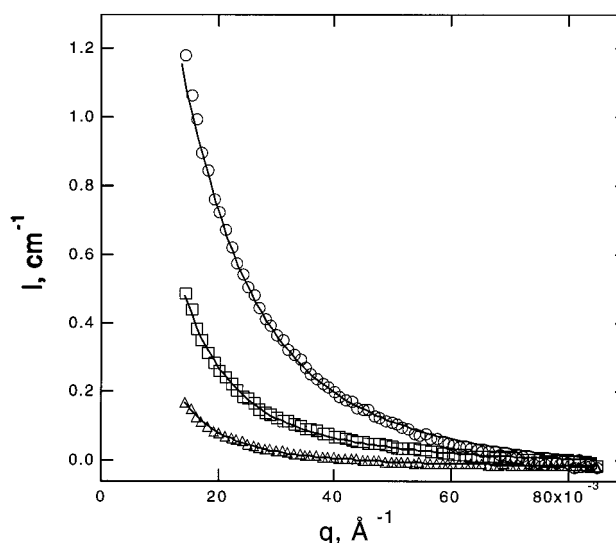


**Figure 1.** SANS scattered intensity,  $I(q)$ , plotted versus the scattering vector  $q$  for PVP in ethylene glycol- $d_6$  for three different polymer concentrations: (O) 10 g/L; (□) 4.2 g/L; (Δ) 1.2 g/L. The solid lines are the result of Debye function fits to the data.

**Table 1.** Values of Radius of Gyration of Neutral PVP Extracted from Debye Function Fits to SANS Data as Seen in Figure 1

concentration, g/L	$R_g$ , nm
1.2	$16 \pm 0.9$
4.2	$14 \pm 1.3$
10	$10 \pm 1.2$

solutions.<sup>20</sup> Also shown in Figure 1 are Debye function fits to the data based on the formula

$$I(\theta) = A + \left(\frac{B}{x^2}\right) (e^{-x} - 1 + x) \quad (1)$$

where  $x = q^2 \langle R_g^2 \rangle$  and  $R_g^2$  is the mean square radius of gyration,  $A$  is an incoherent baseline parameter, and  $B$  is an arbitrary intensity scaling factor. The results of nonlinear curve fitting for  $A$ ,  $B$ , and  $R_g^2$  are displayed in Table 1. The Debye function fits the data quite well over the range of scattering angles and the values of  $R_g$  determined from eq 1 agree well with those for a vinyllic polymer of this Mw in a good solvent.<sup>26</sup>

The introduction of charges to the PVP chain dramatically alters the scattering profiles. Figure 2 displays the SANS profile of PMVP in EG- $d_6$  with no added salt at concentrations ranging from 2 to 23 g/L. Each curve shows one broad maximum whose position is a strong function of concentration; the peak moves to higher  $q$  with increasing concentration. At  $q$  values below  $0.02 \text{\AA}^{-1}$ , a sharp upturn is clearly evident. These are common features of small angle scattering from aqueous polyelectrolyte solutions and, to our knowledge, the first such observation in nonaqueous solutions. Thus, in a solvent for which there are no hydrophobic interactions, the characteristic broad maximum and sharp low  $q$  upturn persist.

As mentioned earlier, similar features have been seen for weakly charged aqueous polyelectrolyte solutions.<sup>15,18</sup> In those systems, the maximum was taken as evidence of microphase separation of polymer rich domains and analyzed under the framework of the BE model. The present study is not for a weakly charged system which typically refers to polymers with charge densities lower

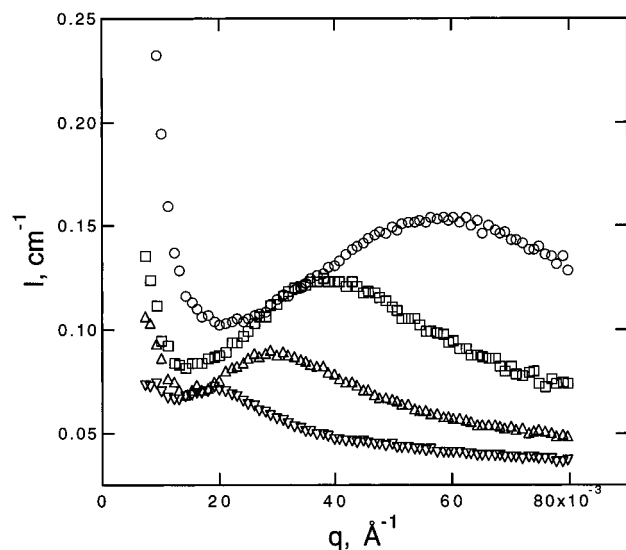


**Figure 2.** SANS scattered intensity,  $I(q)$ , plotted versus the scattering vector  $q$  for PMVP in ethylene glycol- $d_6$  for four different polymer concentrations: (○) 23 g/L; (□) 8.1 g/L; (△) 4.2 g/L; (▽) 2.2 g/L.

than 10%. The charge densities of the polymers involved in this study are 45%. This is more than sufficient to reach the limit of charge density for Manning counterion condensation to occur.<sup>27</sup> This is particularly true for ethylene glycol in which the counterion condensation limit is reduced by approximately a factor of 2 compared to its value in water. Condensation theory predicts that high Coulombic intrachain repulsions are moderated by condensation of counterions equivalent to a fraction of the available ionizable groups. The actual bare charge on a polyelectrolyte chain is reduced to a more stable, lower effective level. In water, this value is equivalent to a linear charge spacing or Bjerrum length,  $l_B$ , of 0.71 nm which corresponds to about 35% of the monomers for a vinyl-based polymer. Because of the lower dielectric constant, the linear charge spacing increases to 1.49 nm in EG, which leads to an effective charge density of about 17% for this system. An important extension of this work, which is now in progress, is to characterize the effect of charge density in samples with charge densities of 10% and lower.

In Figure 3, SANS profiles from the same polymer in  $D_2O$ , which is a poor solvent for the backbone, are shown for a similar concentration range. The profiles have identical qualitative features to the EG- $d_6$  solutions: a single broad maximum which is strongly dependent on concentration and a steep upturn at low values of  $q$ . These observations, coupled with the ordinary scattering observed for the neutral chains in EG- $d_6$ , provide compelling evidence that electrostatic interactions, not hydrophobic interactions, are responsible for the solution structure giving rise to the unusual scattering.

Some previous investigations<sup>18</sup> have taken the upturn at low  $q$  as evidence of incipient macroscopic demixing promoted by hydrophobic interactions in aqueous solutions, yet we see the same low  $q$  scattering behavior in our system without hydrophobic interactions. It is evident that the upturn seen at low angles in our SANS measurements is not caused by hydrophobic interactions or phase separation. Recent static light scattering studies<sup>12,14</sup> on aqueous polyelectrolyte solutions, have shown that large scale structures are present. These structures were demonstrated to be much larger than

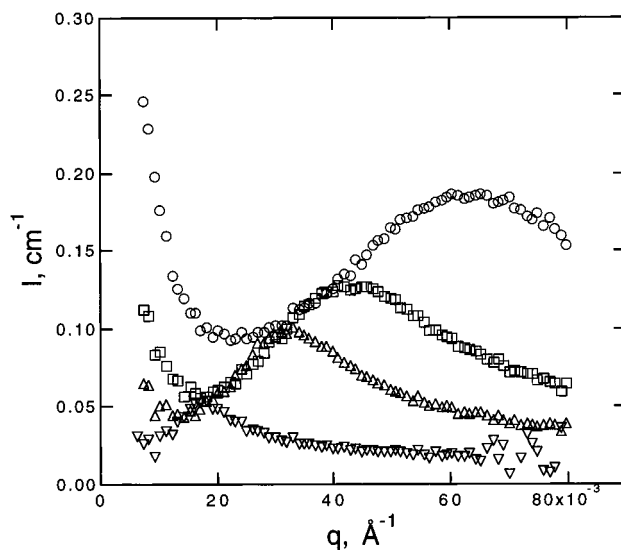


**Figure 3.** SANS scattered intensity,  $I(q)$ , plotted versus the scattering vector  $q$  for PMVP in deuterium oxide for four different polymer concentrations: (○) 22 g/L; (□) 8.8 g/L; (△) 4.5 g/L; (▽) 2.2 g/L.

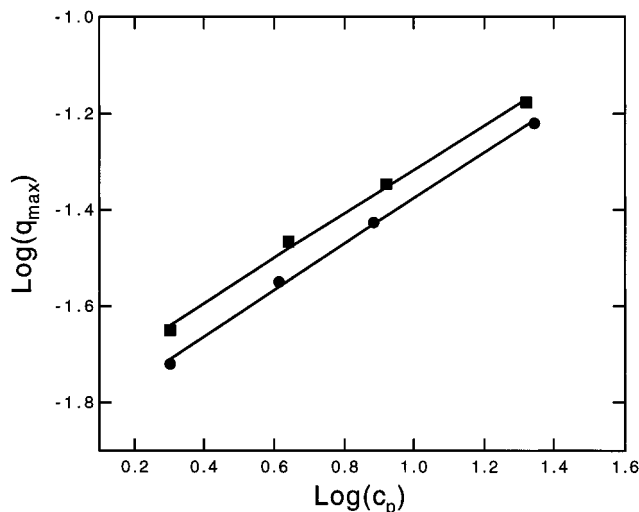


**Figure 4.** log-log plot of  $q_{\max}$  versus concentration (g/L) of PMVP in (●) ethylene glycol and (■) deuterium oxide. Solid lines are least-squares fits to the data which yield slopes of 0.48 for the EG solutions and 0.46 for the  $D_2O$  solutions.

the size of single chains and were therefore attributed to multichain clusters. Because light scattering probes smaller  $q$  values than SANS, sizes of the domains were quantified, yielding  $R_g$  values ranging from 60 to 100 nm.<sup>14</sup> Although the present SANS study does not include  $q$  values low enough for analysis of  $R_g$ , the upturn at our lowest angles is consistent with the observation of large domains in light scattering. Thus, we suggest the upturn at low  $q$  in our SANS measurements provides further evidence for the presence of multichain domains which persist on finite time scales. The nature of the low  $q$  data will be addressed more fully in future work.

Figure 4 shows the concentration dependence of the broad maximum in both  $D_2O$  and EG- $d_6$  on a log-log plot along with a linear least-squares fit to the data. In EG- $d_6$  and  $D_2O$  the scaling behavior is nearly identical,  $q_{\max} \propto c_p^{0.46 \pm 0.02}$  for the  $D_2O$  solutions and  $q_{\max} \propto c_p^{0.48 \pm 0.02}$  for the EG solutions, which is consistent with previous investigations. Quantitatively, the values of the scaling exponents for the EG- $d_6$  and  $D_2O$  solutions,  $0.46 \pm 0.02$  and  $0.48 \pm 0.02$ , respectively, are in good

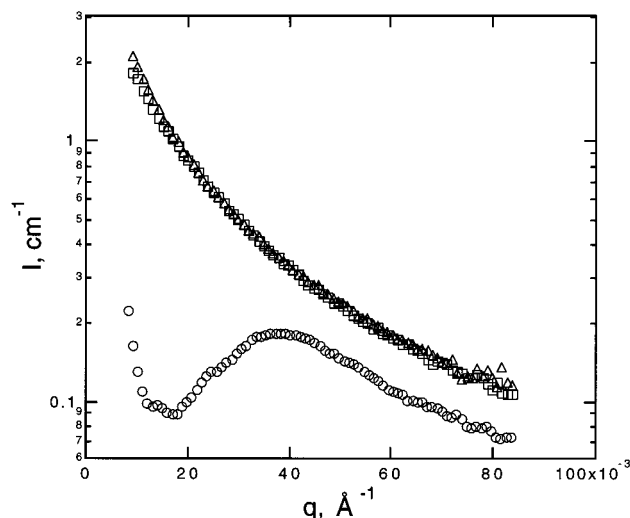


**Figure 5.** SANS scattered intensity,  $I(q)$ , plotted versus the scattering vector  $q$  for (○) PMVP in ethylene glycol- $d_6$  with zero added salt, for (□) PMVP in ethylene glycol- $d_6$  with excess NaCl, and for (Δ) PVP in ethylene glycol- $d_6$ .

agreement with predictions of both the scaling and lattice models.<sup>28–31</sup> In the scaling approach<sup>28–30</sup> a semidilute polyelectrolyte solution is pictured as a dense packed assembly of blobs of radius  $\xi$ , corresponding to the correlation length. This isotropic model is characterized in reciprocal space by a maximum in the scattering profile whose position,  $q_{\max}$ , varies with the inverse of the correlation length and therefore scales with the polymer concentration,  $c_p$ , as  $c_p^{1/2}$ . The lattice model<sup>31</sup> considers the existence of ordered structures in solution and also predicts the  $c_p^{1/2}$  scaling of the broad maximum. In this approach, a parallel orientation of aligned cylinders or polyelectrolyte rods is proposed. The peak position is then given by the Bragg condition  $q_{\max} = 2\pi/d$ , where  $d$  is the intercylinder distance. For a lattice of rodlike molecules, a  $q_{\max} \sim c_p^{1/2}$  relation results. It is important to note that neither scaling nor the lattice model predicts the presence of long wavelength concentration fluctuations, which is evidenced in our data by the upturn at low wavevector.

At equivalent polymer concentration, the actual magnitude of  $q_{\max}$  does shift when the solvent is changed from EG- $d_6$  to  $D_2O$ . We cannot distinguish if this small shift is related to an increase of dielectric constant, and thus effective charge density, or a reduction in solvent quality for the backbone. Further SANS investigations on this system using solvents that are good for the backbone but have different dielectric constants are currently in progress. These experiments coupled with the influence of charge density on peak position could answer this question.

To further demonstrate that the unusual small angle neutron scattering behavior is electrostatic in nature, three separate ethylene glycol- $d_6$  solutions were prepared: a neutral chain solution, a polyelectrolyte solution without added salt, and a polyelectrolyte solution with an excess amount of salt. All solutions were prepared at the same monomer molar concentration of 0.070 mol/L. Figure 5 displays scattering profiles for the neutral chain PVP, the salt-free methyl-substituted PVP polyelectrolyte, and the polyelectrolyte with a 2-fold equivalent of sodium chloride, all on an absolute intensity scale. Clearly, the addition of excess salt to the low ionic strength solution causes the disappearance of the broad maximum and the observation of a scattering

profile that is nearly identical to the neutral chain. The added salt effectively screens long range electrostatic interactions such that the solution structure is again dominated by the chain itself. To our knowledge, this is the first clear demonstration of the small angle scattering of a neutral polymer compared to its covalently bonded polyelectrolyte analogue, both in high and low salt conditions.

At low  $q$  values, the overall scattering intensity for the polyelectrolyte is 1 order of magnitude lower than that of the other samples. This may be understood by considering the large osmotic pressure of low ionic strength polyelectrolytes that serve to suppress density fluctuations. The osmotic compressibility can be related to scattering intensity extrapolated to  $q = 0$  by<sup>32</sup>

$$S(0) \approx k_B T \frac{\partial c}{\partial \Pi} \quad (2)$$

where  $k_B$  is Boltzmann's constant,  $T$  the temperature,  $\Pi$  the osmotic pressure, and  $c$  the monomer concentration. It can be seen from eq 2 that the incompressibility of polyelectrolyte solutions causes  $S(q \rightarrow 0)$  to be small and for there to be weak forward scattering. We stress that this phenomenon diminishes but does not preclude the presence of long wavelength density fluctuations, which are clear from our data as well as in the dynamic light scattering data.<sup>24</sup> At high ionic strengths, density fluctuations are no longer suppressed and the scattering intensity is expected to resemble the neutral chain behavior. Qualitatively, this behavior is depicted by the data presented in Figure 5. This experiment provides additional evidence that the unusual scattering observed for low ionic strength polyelectrolyte solutions is electrostatic in origin.

As mentioned earlier, previous investigators used BE theory to interpret the SANS from aqueous polyelectrolyte solutions. Strictly speaking, the application of BE theory should fail for analysis of the scattering from PMVP/EG- $d_6$  solutions. The model was developed for charged macromolecules in a solvent which is marginal or poor for the backbone. This is not the case for PMVP in EG- $d_6$ . In the following discussion, it is demonstrated that if the steep upturn at low angles is ignored, the BE scattering function fits our data quite well, even when microphase separation from hydrophobic interactions is not present.

The BE model treats a polyelectrolyte solution as a three-component system comprised of macroions, counterions, and solvent. The basis of the theory starts from a weakly charged single polyelectrolyte chain in salt-free solution following the concept of "electrostatic blobs".<sup>28,29,33</sup> In this model, the polyelectrolyte chain is described as a rod of connected chain subunits or electrostatic blobs within which electrostatic interactions are considered weak perturbations. The consequence is that the local properties of the chain are only weakly influenced by electrostatic forces and dominated by monomer-solvent interactions. In the random phase approximation (RPA) representation of a semidilute solution, the correlation radius is directly related to this blob size and thus the monomer-solvent interaction parameter  $\chi$ . In the absence of charged monomers, a polymer solution of this type demixes into macroscopic polymer-rich and polymer-poor phases. However, for polyelectrolytes this separation would result either in large unscreened electric charges in the polymer-rich phase or in the localization of free counterions into the polymer phase to neutralize the bare charge, which is

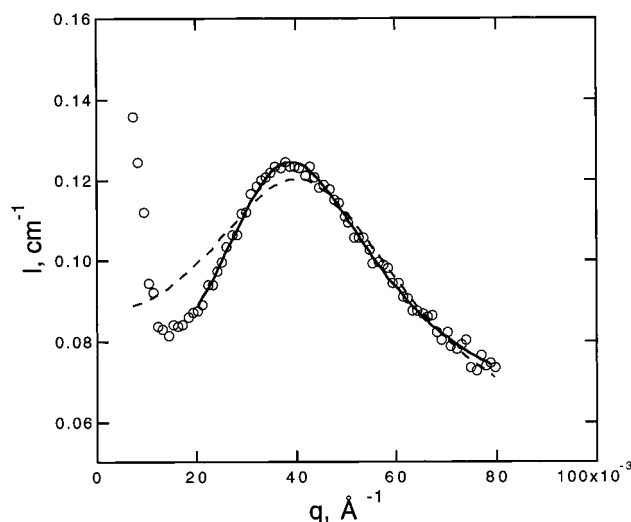


**Figure 6.** SANS scattered intensity,  $I(q)$  plotted versus the scattering vector  $q$  for 8.1 g/L PMVP in ethylene glycol- $d_6$ . The dashed line is the result of a BE function fit to all of the data, including the steep upturn at low  $q$ . The solid line is the result of a BE function fit to the data, excluding the low  $q$  data.

entropically unfavorable. It is this competition of forces which may lead to the formation of stable oppositely charged polymer-rich and polymer-poor microdomains. Using RPA formalisms, the calculated structure factor is given by

$$S(x) = C_1 \frac{(x^2 + s)}{(x^2 + s)(x^2 + t) + 1} \quad (3)$$

where  $C_1$  is a scaling constant,  $x$  is the reduced scattering vector,  $t$  is the reduced temperature, and  $s$  is the reduced charge concentration. The reduced scattering vector is defined as  $x = r_0 q$ , where  $r_0$  represents the characteristic scale of electrostatic screening caused by the polymer coil and is given by

$$r_0 = a \left( \frac{48\pi l_B}{a} \phi \alpha^2 \right)^{-1/4} \quad (4)$$

where  $a$  is the segment length,  $l_B$  the Bjerrum length,  $\alpha$  the charge density, and  $\phi$  the polymer volume fraction. The reduced charge concentration  $s$  is defined in terms of the Debye screening length, i.e.,  $s = \kappa^2 r_0^2$ . The reduced temperature stands for the solvent quality, good when  $t > 0$ , poor when  $t < 0$  and is defined as

$$t = 12 \left( \frac{r_0}{a} \right)^2 \left[ (1 - 2\chi) + \left( \frac{3B_3}{a^3} \right) \phi \right] \quad (5)$$

where  $\chi$  is the Flory interaction parameter and  $B_3$  the third virial coefficient.

Figure 6 shows the results of BE fitting using eq 3 with  $C_1$ ,  $s$ ,  $t$ , and  $r_0$  as adjustable parameters. The open circles are the small angle neutron scattering data from a 8.1 g/L solution of PMVP-Cl in ethylene glycol- $d_6$  and the dashed line is the fit to the full data set. Clearly, the fit is poor because of the low-angle scattering where the steep upturn dominates. It has been found that if the low-angle data are ignored or arbitrarily subtracted from the scattering profile, fits can be quite reasonable.<sup>18</sup> The solid line shows the results of BE fitting to the data. The fit procedure did not include data below  $q \sim 0.02 \text{ \AA}^{-1}$ . In this case, which must be considered somewhat arbitrary, the curve adequately represents

the data, with the shape, position, and height of the maximum surprisingly well depicted. Thus, Figure 6 presents an intriguing result and provides further evidence that long range electrostatic interactions must be considered dominant in polyelectrolyte systems. Earlier investigators used the physical picture of hydrophobic monomer-solvent interactions to interpret the formation and dimensional change of a characteristic correlation length in polyelectrolyte solutions. As is demonstrated in this paper, poor polymer-solvent interactions are not required to exhibit typical polyelectrolyte behavior. Therefore hydrophobicity cannot be the primary factor controlling the correlation length scale and, consequently, the maximum observed at intermediate wavevector. Even for solutions containing charged monomers, neutral monomers, counterions, and solvent molecules, electrostatics overwhelm the local monomer-solvent and monomer-monomer interactions. We suggest that a more universal model to describe the physics of charged macromolecular solutions must be based on strong monomer-monomer correlations promoted by long range electrostatic interactions.

## Conclusion

In this work, we show that the qualitative nature of static scattering measurements on polyelectrolyte solutions with and without the presence of hydrophobic interactions is equivalent. For both of these cases, we see the same concentration scaling of the broad peak at finite  $q$ . It is concluded that hydrophobic interactions or a phase separation process are not required to model the structure of salt-free polyelectrolyte solutions. Changing the solvent from water to ethylene glycol does introduce a small shift in peak position, which we attribute to either a change in solvent quality or effective charge density. The scattering from the equivalent neutral chain shows no maximum at finite  $q$  or sharp upturn at low  $q$ , in dramatic contrast to any of the polyelectrolyte solutions. In the low ionic strength polyelectrolyte solutions, structures larger than single chains are indicated by the upturn in small angle neutron scattering and are interpreted in terms of multichain domains. Such domain structures are consistent with previous observations by static light scattering. In these same solutions, structure on a much shorter length scale is also evident by the peak in SANS at finite  $q$ . A model used to explain the physics of such solutions must explain all these features, and no current model meets this challenge. Furthermore, the scattering observed from the polyelectrolyte chain in a solution containing an excess amount of low molecular weight salt is virtually identical to the neutral chain scattering. This strongly suggests that the physics which controls the unusual scattering observed for low ionic strength polyelectrolyte solutions is electrostatic in nature. Only if the data at lowest angles is ignored can the structure factor which claims to model scattering from weakly charged polyelectrolytes in a poor solvent fit our scattering data, and this occurs despite the absence of hydrophobic interactions.

**Acknowledgment.** We are grateful to Dr. Charles C. Han and Dr. Jack F. Douglas for their helpful discussions and critical reading of the manuscript.

## References and Notes

- (1) *Polyelectrolytes: Science and Technology*; Hara, M., Ed.; Marcel Dekker: New York, 1993.

- (2) *Macro-ion Characterization*; Schmitz, K., Ed.; American Chemical Society: Washington, DC, 1994.
- (3) Lin, S. C.; Lee, W. I.; Schurr, J. M. *Biopolymers* **1978**, *17*, 1041.
- (4) Cotton, J. P.; Moan, M. *J. Phys. (Paris)* **1976**, *37*, 75.
- (5) Moan, M. *J. Appl. Cryst.* **1978**, *11*, 519.
- (6) Nierlich, M.; Williams, C. E.; Boue, F.; Daoud, M.; Farnoux, B.; Jannick, G.; Picot, C.; Moan, M.; Wolff, C.; Rinaudo, M.; de Gennes, P. G. *J. Phys. (Paris)* **1979**, *40*, 701.
- (7) Schmitz, K. S.; Lu, M.; Gauntt, J. *J. Chem. Phys.* **1983**, *78*, 5059.
- (8) Drifford, M.; Dalbiez, J. P. *J. Phys. Chem.* **1984**, *88*, 5368.
- (9) Ise, N.; Okubo, T.; Kunugi, S.; Matsuoka, H.; Yamamoto, K.; Ishii, Y. *J. Chem. Phys.* **1984**, *81*, 3294.
- (10) Ise, N. *Angew. Chem., Int. Ed. Engl.* **1986**, *25*, 323.
- (11) Sedlak, M.; Konak, C.; Stepanek P.; Jakes, J. *Polymer* **1987**, *28*, 873.
- (12) Forster, S.; Schmidt, M.; Antonietti, M. *Polymer* **1990**, *31*, 781.
- (13) Matsuoka, H.; Schwahn, D.; Ise, N. *Macromolecules* **1991**, *24*, 4227.
- (14) Sedlak, M.; Amis E. J. *J. Chem. Phys.* **1992**, *96*, 817.
- (15) Moussaid, A.; Schosseler, F.; Munch, J. P.; Candau, S. J. *J. Phys. II* **1993**, *3*, 573.
- (16) Boué, F.; Cotton, J. P.; Lapp, A.; Jannick, G. *J. Chem. Phys.* **1994**, *101*, 2562.
- (17) Milas, M.; Rinaudo, M.; Duplessix, R.; Borsali, R.; Lindner, P. *Macromolecules* **1995**, *28*, 3199.
- (18) Shibayama, M.; Tanaka, T. *J. Chem. Phys.* **1995**, *102*, 9392.
- (19) Essafi, W.; Lafuma, F.; Williams, C. E. *J. Phys. II* **1995**, *5*, 1269.
- (20) Debye, P. *J. Phys. Colloid Chem.* **1947**, *51*, 18.
- (21) Borue, V. Yu.; Erukhimovich, I. Ya. *Macromolecules* **1988**, *21*, 3240.
- (22) Joanny, J. F.; Leibler, L. *J. Phys. (Paris)* **1990**, *51*, 545.
- (23) Hodgson, D. F.; Amis, E. J. *J. Chem. Phys.* **1989**, *91*, 2635.
- (24) Ermi, B. D.; Amis, E. J. *Macromolecules* **1996**, *29*, 2703.
- (25) Certain commercial material and equipment are identified in this publication in order to specify adequately the experimental procedure. In no case does such identification imply recommendation by the National Institute of Standards and Technology nor does it imply that the material nor equipment identified is necessarily the best available for this purpose.
- (26) *Polymer Handbook*; Brandrup, J., Immergut, E. H., Eds.; Wiley: New York, 1989.
- (27) Manning, G. S. *J. Chem. Phys.* **1969**, *51*, 924.
- (28) de Gennes, P. G.; Pincus, P.; Velasco, R. M.; Brochard, F. *J. Phys. (Paris)* **1976**, *37*, 1461.
- (29) Pfeuty, P. *J. J. Phys., Colloq. C2* **1978**, *39*, 149.
- (30) Dobrynin, A. V.; Colby, R. H.; Rubinstein, M. *Macromolecules* **1995**, *28*, 1859.
- (31) Lifson, S.; Katchalsky, A. *J. Polym. Sci.* **1954**, *13*, 43.
- (32) de Gennes, P. G. *Scaling Concepts in Polymer Physics*; Cornell University Press: Ithaca, NY, 1979.
- (33) Khokhlov, A. R. *J. Phys. A: Math. Gen.* **1980**, *A13*, 979.
- (34) According to ISO 31-8, the term "molecular weight" has been replaced with "relative molecular mass", symbol  $M_r$ . Thus, if this nomenclature and notation were followed in this publication, one would write  $M_{r,n}$ , instead of the historically conventional  $M_n$  for the number average molecular weight, with similar changes for  $M_w$ ,  $M_z$ , and  $M_v$ , and it would be called the "number average relative molecular mass". The conventional notation, rather than the ISO notation, has been employed for this publication.

MA970494T